ASEAN
Journal of Scientific and Technological Reports
Online ISSN:2773-8752

Research article

Risk Assessment and Geospatial Mapping of Ammonia Transportation Hazards: A Case Study of Thungsong, Thailand

Pisit Kolsaman[1], Supabhorn Yimthiang[2], Preeda Sansakorn[3], Junjira Mahaboon[4*]

[1] School of Public Health, Walailak University, Thaiburi, Thasala, Nakhon Si Thammarat, 80160, Thailand
[2] School of Public Health, Walailak University, Thaiburi, Thasala, Nakhon Si Thammarat, 80160, Thailand
[3] School of Public Health, Walailak University, Thaiburi, Thasala, Nakhon Si Thammarat, 80160, Thailand
[4] School of Public Health, Walailak University, Thaiburi, Thasala, Nakhon Si Thammarat, 80160, Thailand
* Correspondence: hjunjira@wu.ac.th

Citation:
Kolsaman, P.; Yimthinang, S.; Sansakorn, P.; Mahaboon, J. Risk assessment and geospatial mapping of ammonia transportation hazards: A case study of Thungsong, Thailand *ASEAN J. Sci. Tech. Report.* **2025**, *28*(1), e254894. https://doi.org/10.55164/ajstr.v28i1.254894

Article history:
Received: July 16, 2024
Revised: November 13, 2024
Accepted: November 20, 2024
Available online: February 16, 2025

Publisher's Note:
This article has been published and distributed under the terms of Thaksin University.

Abstract: The transportation of ammonia—a widely used industrial chemical—presents significant risks, including leaks, fires, and explosions. This study aimed to assess the risks of transporting ammonia in the southern part of Thailand and to create a detailed risk evaluation using geospatial methods. We used the Areal Locations of Hazardous Atmospheres (ALOHA) to comprehensively simulate five ammonia accident scenarios: toxic vapor cloud, flammable areas (flash fire and jet fire), boiling liquid expanding vapor explosion (BLEVE), and vapor cloud explosion while risk, severity, and evacuation routes were mapped using ArcGIS software. The simulation results reveal that variations in wind direction influence ammonia spread across different seasons. In summer and winter, the wind direction is northeast, and in the rainy season, it shifts to southwest. In scenario 1, the red zone extends 2,400 meters from the source, with ammonia levels reaching up to 505,000 ppm, while in scenario 2, the red zone spans 368 meters. Explosive hazards (BLEVE and VCE) have ranges of 207 and 310 meters, respectively. While our study provides detailed mapping of ammonia hazard zones, future studies are needed to incorporate socio-economic factors into geospatial analyses to improve evacuation strategies and risk mitigation. Consequently, the maps produced can be utilized as essential decision-making tools in emergency response planning and management, which may reduce the death toll during a disaster in the future.

Keywords: Ammonia transportation accidents; Risk assessment; Risk mapping; ALOHA; Evacuation route map

1. Introduction

The rapid growth of industrial development has escalated the demand for raw materials [1], leading to a substantial increase in the production, distribution, and transportation of hazardous chemicals. In Thailand, approximately 120 million tons of dangerous goods are transported, with trucks being the primary mode of transportation. Some studies in China have shown that approximately 95% of hazardous materials (HAZMAT) are transported from producers to customers by trucks [2, 3]. Around 55% of hazardous materials were transported via roadways [1, 4]. According to previous studies [2, 5], 90% of hazardous materials transportation occurs on highways, intersections,

and along rural and urban roads. The significant risks posed by truck crashes identify them as critical issues in road transportation [1, 6]. Several studies pointed out that the high risk due to transportation activities is comparable to or even more critical than the risk due to fixed installations [7]. The risk associated with various road transportation cases is representative of hazardous materials transported by land in many countries [8]. The same kind of accidental scenarios in terms of frequency and severity may occur in fixed plants and transportation systems. Nevertheless, whether it's an accident or a toxic gas release incident, it can cause heavy casualties and severe economic losses. Additionally, transport accidents may occur close to, and sometimes within, densely populated areas [7, 9]. Transportation activities can provoke major fires, explosions, and toxic release events [10]. Previous studies have predominantly focused on ammonia transportation accidents, primarily emphasizing dispersion, fire, and explosion scenarios. For example, Inanloo and Tansel conducted a study investigating the accidental release of ammonia, predicting the consequences of ammonia transportation [5]. The failure of a 22-ton ammonia storage tank truck in Dakar [11].

Ammonia is in a gas or liquid state under pressure. If under normal pressure conditions, it will be a colorless gas with a strong pungent odor [5, 12-14]. Although ammonia becomes a liquid at -33.4°C under pressure and low temperatures, it is stable at normal temperatures and lighter than air [2, 14, 15]. Due to these properties, accidents can be frequent annually. This is mainly caused by trucks' transportation of hazardous materials, which serves as the primary source of these incidents. Health effects are due to the inhalation of ammonia released into the atmosphere, which is the main route of exposure [2, 15, 16]. The health risk assessment involves toxicology in evaluating ammonia exposure, including routes/pathway concentration of ammonia entering the body dose, frequency of exposure, duration of exposure, and characteristics of the exposed population. Ammonia toxicity occurs when sensitive individuals are exposed to external ammonia sources through ingestion, inhalation, or direct contact with the skin or eyes. Ammonia toxicity has both acute and chronic adverse effects on patients. For example, exposure to levels exceeding 30 ppm results in immediate irritation of the nose and throat [17, 18]. Effects on various systems in the body effects on the respiratory: ammonia is an irritant to the human upper respiratory tract. Other effects of ammonia can range from severe irritation to the eyes, nose, and throat and difficulty breathing, pulmonary edema, pink frothy sputum, skin burns blisters, and severe burns on the skin and in the mouth, throat, lungs, and eyes, leading to death [12, 15, 19-24]. The effects of ammonia exposure and decreased lung function have also been evaluated [25]. High ammonia concentrations can acutely affect the cardiovascular system in humans, causing increased pulse, elevated blood pressure, bradycardia, and even cardiac arrest [17, 26, 27]. Some studies indicate that exposure to ammonia concentrations above 2,500 ppm for approximately 30 seconds can be fatal [12].

Although assessing the risk of road transport crashes involves considering the probability of occurrence and the severity of their consequences, ammonia transport truck crashes remain unpredictable. Studies have investigated potential events like collisions, overturning, tank ruptures, and the leakage or ignition of substances inside, which can cause fires or explosions. The consequences of toxic release and blast overpressure were modeled for various worst-case scenarios of the critical units. Both structural damage and human mortality/injury were converted into economic terms using suitable probability functions, frequency, and cost parameters related to property damage and compensation for fatalities [28]. The ALOHA software is widely used in simulating the spread of chemicals leaking into the air according to the climate, and the chemical characteristics of ALOHA allow for the simulation of various toxic gas emissions situations, calculating the velocity of chemicals coming out of ammonia tanks. Previous studies showed research has been performed using ALOHA software to assess incidents in road transportation [1, 5, 29, 30]. ALOHA has been used in this study to analyze the risk and identify the population under threat. Several studies have been done for ammonia or other chemical risk assessments based on the dispersion model [31, 32]. ALOHA can simulate situations of leakage from storage tanks in cases where there is no ignition, such as toxicity (toxic vapor clouds), flammability, thermal radiation, explosions like boiling liquid into vapor, BLEVEs (Boiling Liquid Expanding Vapor Explosions), fires with flame jets (Jet fires), explosions of vapor cloud explosions and pool fires [33-36].

The variables considered in the simulation are the amount of cloud cover, air temperature, relative humidity, wind speed, and wind direction [23, 37-39]. During the cold season, temperature fluctuations cause

freeze-thaw cycles in bioretention systems, affecting soil structure, permeability, and microbial activity, reducing stormwater and pollutant filtration effectiveness. This accident on the highway can lead to ammonia release, posing a risk to ecosystems by potentially causing eutrophication in nearby waters. Effective management strategies are needed to minimize ammonia leaching and maintain pollutant removal efficiency in regions with freeze-thaw cycles [40, 41]. For ammonia transport, any integration with or impact by bioretention systems designed to manage stormwater and reduce pollutants is unlikely to face freeze-thaw-related challenges in Thailand. Instead, considerations would focus on factors like high rainfall, heat, and runoff management, ensuring that ammonia handling does not lead to contamination risks within these systems. Researchers used ALOHA to spot intended to create an ammonia distribution model [31].

A GIS-based method has been proposed for vulnerable point mapping and application. Maps of the impact toxic threat zone, radiation threat zone, and impact area zone of accident outcome are prepared using ArcGIS. Many studies have presented the integrated applications of ALOHA and GIS as powerful tools for risk assessment and population vulnerability assessment [31, 38, 42, 43]. ALOHA and ArcGIS are integrated in this study. Addressing the knowledge gap of no previous studies on road ammonia transport in this area, our research employs a systematic and evidence-based approach to evaluate the risks and develop comprehensive risk mapping using geospatial tools. The objectives of this study were to evaluate the risks associated with ammonia transportation and develop a comprehensive mapping for risk evaluation using geospatial tools. Therefore, this study focuses on conducting a thorough risk assessment for the transportation of ammonia along national highways. These highways, being vital routes for ammonia transportation and have statistics of accidents many times, might pose potential risks to the vicinity general populations. The novelty of this paper is the integration of the assessment of ammonia transportation accidents and the implementation of risk and evacuation mapping.

2. Materials and Methods

The methodology employed in this study to define the nature and calculate the extent of a possible release of ammonia transportation on the population of Thungsong district, Nakhon Si Thammarat, Thailand, and surrounding a five-step approach applied to five scenarios was illustrated in Figure 1.

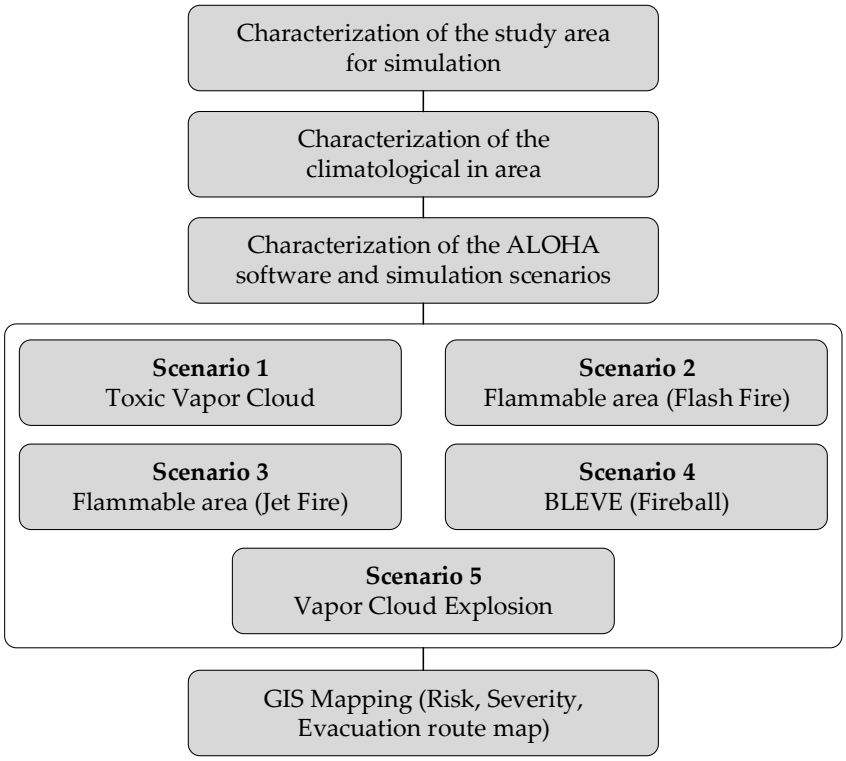

Figure 1. Conceptual framework of research.

2.1 Characterization of the study area for simulation

Ammonia transportation routes pass through Highway No. 41 in Nakhon Si Thammarat province. The Thungsong district was selected in the present study because of the daily ammonia transportation, variety of fuels/hazardous chemicals, and enormous quantities on this highway. The number of ammonia trucks on Nakhon Si Thammarat highways varies based on demand, industrial activity, transport schedules, and regulations. Transportation authorities or logistics companies typically monitor this data. No such study has been conducted on this highway area. Figure 2 and Table 2 show the characteristics of the ammonia emission source and its location in Thungsong, inhabited by 116,757 people and a vulnerability group of 37,720 people.

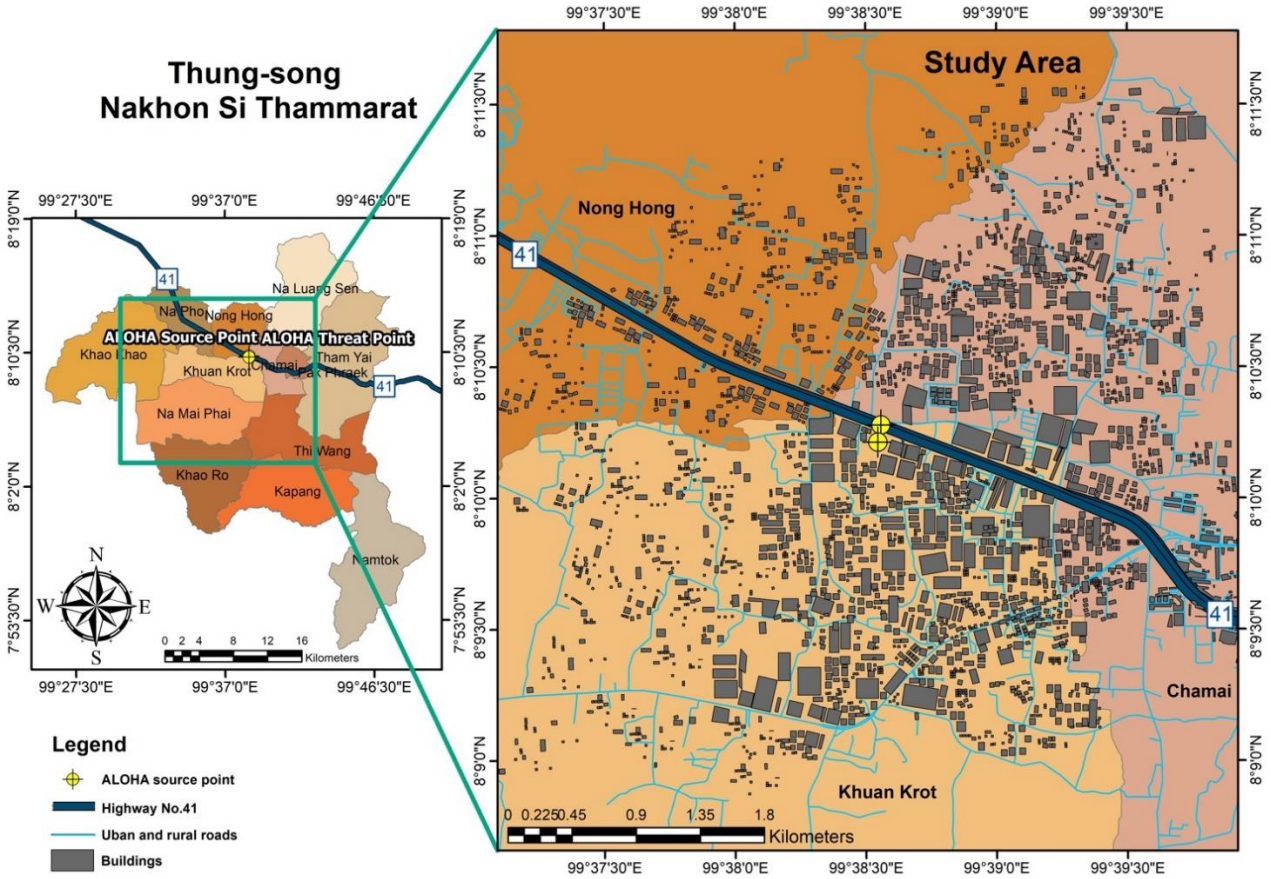

Figure 2 The study area of ammonia transportation routes passes through Highway No. 41 in Nakhon Si Thammarat province.

2.2 Data collection

A survey for data collection on the selected ammonia transport tank was carried out regarding the type of ammonia tanker and and the toxicity of ammonia, considering packaging conditions, diameter, and capacity of the storage tanker. To estimate the risk and effect on the population and surrounding environment, the population data was collected from the population registration statistics (monthly), the Registration Administration Office, the Department of Provincial Administration (2022), and secondary data obtained from the Ministry of Public Health database. The human research project certification document from the Human Research Ethics Committee, Walailak University. For injured analysis, the data regarding a number of populations was collected for the forecast risk and preparedness evacuation plan. For network analysis, the data regarding traffic routing was collected to prepare an evacuation plan.

The weather parameters and meteorological data for the studied area spanning 2020-2024 were collected. The data are provided by the Thai Meteorological Department of Nakhon Si Thammarat province station. For the analysis, meteorological data variables taken into account for this study are air temperature,

wind direction and speed, relative humidity, and cloudiness. For the current and worst situations, several studies estimated the impacts of source release variables (i.e., tank length and diameter) and climatic circumstances (i.e., wind speed, cloud cover, air temperature, and relative humidity) [44]. Nakhon Si Thammarat experiences two monsoon seasons: the southwest monsoon (mid-May to mid-October) with rain from the Indian Ocean and the northeast monsoon (mid-October to mid-February) with cooler winds and occasional rain from China. Thailand's weather is generally divided into summer (mid-February to mid-May), rainy (mid-May to mid-October), and winter (mid-October to February).

2.3 ALOHA software and Consequence analysis

ALOHA was developed by the National Oceanic and Atmospheric Administration (NOAA) and The Environmental Protection Agency (EPA). ALOHA software forecasts the impact or severity of an ammonia release incident. The ALOHA software is a program that has been widely accepted and has suitable features to be used in simulating the spread of chemicals leaking into the air according to the climate and the chemical characteristics of ALOHA allow simulation of various toxic gas emissions situations, calculating the velocity of chemicals coming out of ammonia tanks. Previous studies showed that it has been performed using ALOHA software to assess incidents in road transportation [1, 5, 29, 30] and examine the impact area of the jet fire computed with the ALOHA program [44]. ALOHA has been used in this study to analyze the risk and identify the population under threat. Research has been done on ammonia and other chemical risk assessments using dispersion models [31, 32]. Some studies have simulated dispersion and evaluated the impact on populations and structures [45]. ALOHA can simulate situations of leakage from storage tanks in cases where there is no ignition (toxic vapor clouds), explosions like boiling liquid into vapor, BLEVEs (Boiling Liquid Expanding Vapor Explosions), fires with flame jets (Jet fires), explosions of vapor cloud explosions and pool fires [33] is predicted. The level of concern (LOC) is the reference concentration for assessing the impact during release. The software uses models to describe the dispersion and movement of ammonia and its effects as a spread of ammonia gas, fire, and explosion. Table 3 summarizes the source from the tank and scenarios that ALOHA models. It provided results on threat zones plot, and footprints is a map indicating areas at risk (toxicity, flammability, thermal radiation, or blast force overpressure). In case LOC exceeds in area, people and property are calculated threats. Threat at the point is a graph illustrating the variation of the concentration and time at a point of interest. Text summaries are scenario information, including the physical properties of ammonia, and describe the threat zone and distance. [46] assessment of the consequences of the toxic gas release in major hazards of specified human toxic response for acute exposure to ammonia, etc., expressing susceptibility of population exposure to stressing agents is that of probit analysis.

The scenarios to be studied are selected from the probability that might occur when ammonia is released in the accident storage tanks. Table 1 Consequence scenarios modeling refers to calculating or estimating numerical values. Scenarios involving toxic dispersion, flammable area, boiling liquid expanding vapor explosion (BLEVE), and vapor cloud explosion (VCE) have potential effects and impacts on people in the area inevitably, which often cause a large number of casualties and property losses, environmental health, and safety [47].

Table 1. Expected frequencies (per year) of loss of containment events [48].

Incident cases	Frequency per year
Instantaneous tank car release	3.1E-09
Continuous release of large connection	3.1E-09
Full bore hose	2.2E-06
Leak hose	2.2E-05
Full bore arm	1.7E-08
Leak arm	1.7E-07
Instantaneous storage tank failure	5.0E-07

Table 2. Source and characteristic of assessment point.

Location	Distance from the source (m)	Location name	Characterization
Source	0	Ammonia tank car accident	Ammonia tank car, Stainless or carbon steel, capacity of 9,600 gallons Estimated Weight: 20,360 lbs, Gauges: Level gauges set at 85%, Operating pressure: 100-500 psi, Maximum pressure: 500 psi
Point 1	100	Chamai 1	Possible affected community, LPG gas station: 1, hotel: 1 Temple, community, restaurants, company, village. Maximum 95 inhabitants.
Point 2	350	Chamai 2	Possible affected community, PTT LPG gas station, village, community, restaurants 1,035 inhabitants.
Point 3	500	Chamai 3	Possible affected community, village, community, restaurants 1,848 inhabitants.
Point 4	1,000	Chamai 4	Possible affected community, temple, village, community, restaurants 3,334 inhabitants.
Point 5	1,500	Chamai 5, Khuankrot 1	Possible affected community, village, community, temple, hotel, gasoline station, college, restaurants 3,973 inhabitants.
Point 6	2,100	Chamai 6, Khuankrot 2	Possible affected community, 4,733 inhabitants. Hospital: 1, Medical clinic: 1, School: 2, Market, village, community, restaurants

Table 3. Modeling scenarios of ALOHA software [23, 49].

Source	Toxic scenarios	Fire scenarios	Explosion scenarios
Tank			
Not Burning	Toxic Vapor cloud	Flammable Area (Flash fire)	Vapor Cloud Explosion (VCE)
Burning		Flammable Area (Jet fire)	
Boiling Liquid Expanding Vapor Explosion (BLEVE)		Fireball	

2.4 GIS Mapping

In the case of ammonia transport accidents, mapping involves overlaying relevant data on maps. People's vulnerability maps and risk maps are created using ArcGIS. Overlay with all vulnerable point mapping is performed by overlaying physically and socially vulnerable points in GIS [43]. These maps effectively categorize the studied area into distinct threat zones, disseminate spatial data for assessing risks in each area through mapping, show the distribution of the population who could be exposed to ammonia, and provide a comprehensive visual representation of the risks associated with ammonia transport. Severity, risk, and evacuation route maps are important emergency preparedness and response planning tools. Severity maps display a hazard's potential impact and intensity in a specific area. These maps help emergency management officials and the public understand the level of risk associated with different hazards, such as disasters like chemical spills or industrial accidents. The severity map typically uses color coding or other visual indicators to show areas at high, medium, or low risk of being affected by a hazard. By analyzing severity maps, emergency planners can prioritize resources, make informed decisions, and develop response strategies to mitigate the impact of the hazard. Risk maps provide a comprehensive overview of the likelihood of a hazard occurring in a given area and the potential consequences of that hazard. These maps combine information on the probability of an event with the population's vulnerability and infrastructure in the affected area.

Risk maps are essential for identifying high-risk zones, vulnerable populations, critical infrastructure, and other factors that could influence emergency response and recovery efforts. By analyzing risk maps, decision-makers can allocate resources effectively, implement preventive measures, and enhance community

resilience to disasters. Evacuation route maps are designed to guide individuals and communities in safely evacuating an area in an emergency or disaster. These maps highlight designated evacuation routes, assembly points, shelters, and other important information people need to know to evacuate efficiently and safely. Evacuation route maps ensure orderly and timely evacuations, especially in high-risk areas prone to hurricanes, wildfires, or tsunamis. By familiarizing themselves with evacuation route maps, residents can take proactive measures to protect themselves and their families during emergencies and reduce the risk of injuries or fatalities.

2.5 Population health risk assessment

Health risk assessment involves the general population and vulnerability group considering acute effects such as irritation, respiratory problems, systemic toxicity, and long-term health effects from chronic exposure. Concern number of injured persons are affected by ammonia release. The probability of damage to an exposed population and an individual results in consequences for the population. Proximity to the accident site includes residents within a defined radius of the transportation route and individuals in institutions such as schools, hospitals, temples, and nursing homes near the accident site. These criteria ensure a comprehensive identification of individuals at increased risk during an ammonia transportation accident, enabling targeted protective measures and efficient resource allocation during emergency response planning.

3. Results and Discussion

3.1 Meteorological data in the study area

A variety of factors, both physical and geographical, influence meteorological data. These factors can impact weather patterns, climatic conditions, and atmospheric phenomena, shaping the data collected by meteorological instruments and sensors. Several factors influence the spread of ammonia clouds, including wind speed, temperature, relative humidity, and the extent of cloud cover [4, 23, 37]. The risk of release was assessed by selecting the average values of wind direction, wind speed, and temperature across four seasons [50]. Data on weather and meteorological parameters in the study area during 2020-2024 were collected from the Meteorological Department of Nakhon Si Thammarat province station. The weather variables were averaged.

3.1.1 Air temperature

The annual average air temperature is 29.74°C during the period. This study categorized the seasonal summer (February-May) and rainy season (June-September). The highest air temperature is in April (37°C). The maximum air temperature in the winter (October-January) is 35°C, while the lowest monthly average occurs in December and January at 23.8°C and 23.25°C, respectively. December and January are the coldest months when the minimum temperatures of 22°C and 23°C are recorded. Atmospheric stability class E represents slightly stable atmospheric stability conditions.

3.1.2 Wind direction and wind speed

The wind direction in summer and winter is southwest, with speeds of 4.1 miles per hour and 3.76 miles per hour, respectively (as measured at the height of 10 meters by a fixed meteorological tower at the site). In the rainy season, the wind will be in the northeast direction and wind speed of 3.8 mph. Therefore, the worst-case scenario study chose low wind speeds. Low wind speeds can cause the spread of ammonia in the air to last longer and have a high concentration compared to high and variable wind speeds. Ammonia dispersion vapor cloud will move in a downwind direction and spread in a crosswind. Dispersion calculations provide an estimate of the area affected. The modeling of ammonia dispersion involves predicting the movement and spread of ammonia when it leaks into the atmosphere. Typically, the dispersion occurs in the downwind direction or follows the same path as the wind, and the increase in wind speed reduces the diffusion height of the ammonia gas cloud in the downwind direction [20].

3.1.3 Relative humidity

The relative humidity maximum value is 100% in November. The annual average relative humidity maximum is 89.44%. Normally, the southern region of Thailand has a hot and humid climate, and there is a lot of rain even in the hot weather. On the other hand, in this study, the minimum relative humidity was chosen because low humidity will prevent the diffusion of ammonia while maintaining a high concentration

in the atmosphere and does not dilute ammonia. Therefore, the study obtained the values of the more severe variables in the simulation. The summer (February-May) and rainy season (June-September) are 39%RH and 52%RH, respectively. But in winter (October-January), it is 62%RH.

3.1.4 Cloud cover

The sky is over half covered by clouds during June-September, with 7-tenths in the rainy season. In summer and winter, cloud cover averages 5-tenths, while the sky in January-April does not have cloud cover.

Table 4. Variable meteorological data and model of simulation ALOHA software.

Variable	Summer (Feb-May)	Rainy (Jun-Sep)	Winter (Oct-Jan)
Temperature; °C	37	37	35
Relative Humidity; %RH	39	52	62
Wind speed: mph	4.10	3.80	3.76
Wind direction; degree	NE	SW	NE
Cloud cover; %	50%	70%	50%
Model of release	Tank release	Tank release	Tank release
End Time	60 minutes	60 minutes	60 minutes

3.2 Condition for the ALOHA software

The study used parameters suitable to simulate the worst-case scenario, considering meteorological variations between seasons. For the meteorology variables, average values were used as the data for input to software over the five years considered (2020-2024), which was low. The following meteorology parameters allow estimating the dispersion, heat radiation, and overpressure (blast force) of the ammonia: air temperature, wind direction and wind speed, relative humidity, and cloud cover use the average values (maximum values for air temperature and minimum values for wind speed and humidity).

- The researcher selects the dispersion, fire, and explosion models based on the released ammonia and the condition under which the probability leak occurs.
- The leak is from a hole in a horizontal cylindrical tank.
- Tank Diameter: 6 feet.
- Tank length: 45.4 feet.
- Tank Volume: 9,600 gallons
- A tank contains liquid and an internal temperature of 35°C
- Chemical Mass in Tank: 19.9 tons; the tank is 85% full.
- Circular Opening Diameter: 4 inches.
- An opening is 10 inches from the tank bottom.
- Max Average Sustained Release Rate: 10,900 kilograms/minute (averaged over a minute or more).
- Total amount Released: 16,970 kilograms.
- AEGL-1 (60 min): 30 ppm
- AEGL-2 (60 min): 160 ppm
- AEGL-3 (60 min): 1,100 ppm
- Lower Explosive Limit (LEL): 60% 90,000 ppm (Flame Pockets).
- Lower Explosive Limit (LEL): 10% 15,000 ppm.
- Thermal radiation 10.0 kW/(m^2): potentially lethal within 60 seconds.
- Thermal radiation 5.0 kW/(m^2): 2nd degree burns within 60 seconds.
- Thermal radiation 2.0 kW/(m^2): pain within 60 seconds
- Overpressure (blast force): 8.0 psi = destruction of buildings
- Overpressure (blast force): 3.5 psi = serious injury likely
- Overpressure (blast force): 1.0 psi = shatters glass
- Note: The chemical escaped as a mixture of gas and aerosol (two-phase flow).

3.3 Analysis of ammonia release for five scenarios

3.3.1 Scenario 1: toxic vapor cloud modeling of ammonia

This scenario aims to determine concentration estimates at the point downwind, distances of the toxic threat zone, and the direction of the toxic ammonia cloud that affected people's vicinity. Figure 3 illustrates the plot of the toxic ammonia cloud's toxic threat zones in case of a transportation accident release. The X-axis indicates the distance from the source to the affected point, and the Y-axis is the width of the toxic cloud. Category three plotted areas (indicated by different colors: red, orange, and yellow zone) represent ammonia exceeding the LOC values and wind direction confidence lines. The red zone shows the expected concentrations equal to 1,100 ppm or above, which corresponds to Acute Exposure Guideline Levels (AEGL-3) (the airborne concentration, expressed as parts per million (ppm) or milligrams per cubic meter (mg/m^3), of a substance above which it is predicted that the general population, including susceptible individuals, could experience life-threatening health effects or death). In the orange zone, the area of ammonia concentration exceeds 160 ppm, which corresponds with AEGL-2 (the airborne concentration (expressed as ppm or mg/m^3) of a substance above which it is predicted that the general population, including susceptible individuals, could experience irreversible or other serious, long-lasting adverse health effects or an impaired ability to escape). In the yellow zone, the ammonia concentration is 30 ppm, which is the AEGL-1, the airborne concentration (expressed as ppm or mg/m^3) of a substance above which it is predicted that the general population, including susceptible individuals, could experience notable discomfort, irritation, or certain asymptomatic nonsensory effects. However, the effects are not disabling and are transient and reversible upon cessation of exposure.

All three tiers (AEGL-1, AEGL-2, and AEGL-3) used for exposure periods of 60 minutes are selected by the software automatically. ALOHA will provide the AEGL values with a 60-minute exposure duration as the default toxic LOCs. Even though AEGLs are available for five exposure durations, only the 60-minute AEGLs are provided in ALOHA (because it models the release for 60 minutes from the start time). Acute Exposure Level Guidelines (AEGLs) are used by emergency planners and responders all over the world to help them deal with uncommon, generally accidental, chemical releases into the atmosphere. AEGLS are specified concentrations of airborne pollutants that have the potential to cause health consequences and are intended to protect older adults, children, and other people who may be vulnerable. Notably, during the summer season, the determination of hazard distances based on ERPG-2 [51] revealed the longest distance for ammonia reaching 5,400 meters. The software could contingency plan and analyze the affected population, and it can forecast concentration exposure levels in the affected area.

Table 5. Summary distances of ammonia release in all scenarios.

Scenario	**Distance from the source (m)**								
	Summer			**Rainy**			**Winter**		
	Red	Orange	Yellow	Red	Orange	Yellow	Red	Orange	Yellow
Scenario 1: Toxic Vapor cloud	2,400	4,800	8,900	2,500	4,500	8,900	2,400	4,900	8,900
Scenario 2: Flammable Area (Flash fire)	368	-	893	358	-	889	359	-	888
Scenario 3: Flammable Area (Jet fire)	36	64	110	35	63	108	34	62	107
Scenario 4: BLEVE (Fireball)	207	301	476	204	297	469	204	296	468
Scenario 5: Vapor Cloud Explosion (VCE)	310	364	639	304	359	630	304	360	628

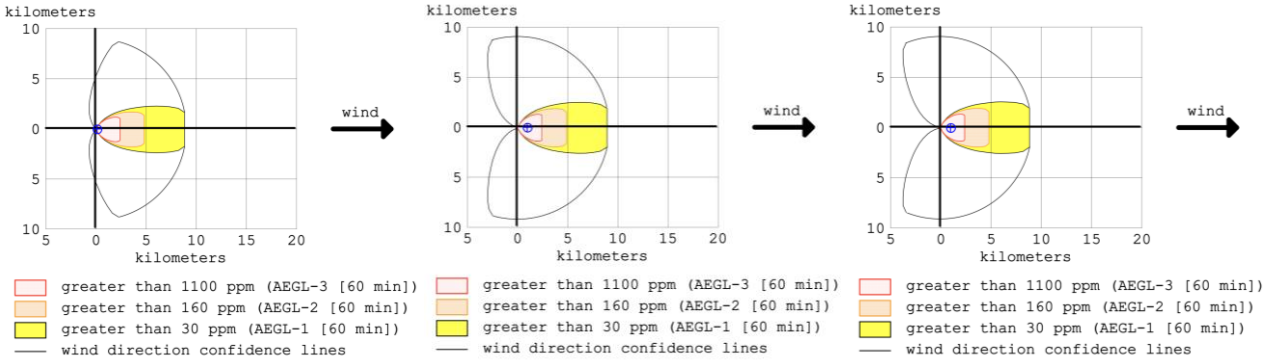

(a) (b) (c)

Figure 3. Footprint ammonia toxic threat zone scenario 1 (a) summer (b) rainy (c) winter.

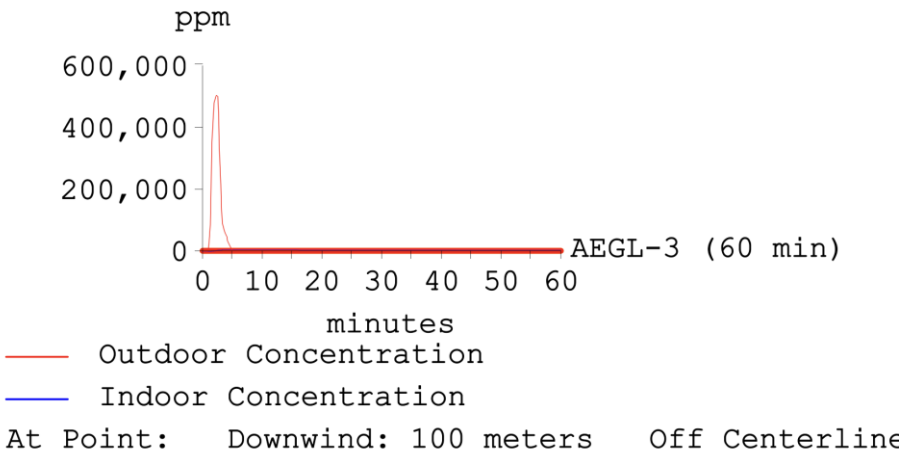

Figure 4a. Concentration at point 100 m. from source.

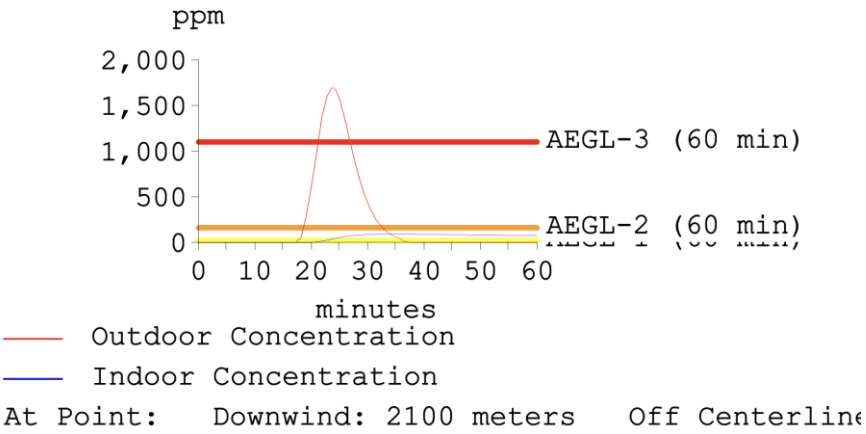

Figure 4b. Concentration at point 2,100 m. from source.

Figures 4a and 4b have concentration at a point in the red zone in the summer season. Figure 4a corresponds to point 1, located 100 meters from the accident source. After 5 minutes, the accident caused an indoor concentration exceeding the AEGL-3 at 6,270 ppm. During the first 5 minutes of the accident, a maximum outdoor concentration exceeding 505,000 ppm is likely to be exposure that can cause immediate lethal. Location point 6 is located at a distance from downwind 2,100 meters from the accident source, as shown in Figure 4b. This area is in part of the red zone, with indoor concentration exceeding AEGL-1 at 94.6 ppm and maximum outdoor concentration exceeding AEGL-3 level at 1,680 ppm are predicted 25 minutes after the incident, which it is predicted that the general population, including vulnerable individuals, could

face life-threatening health consequences or death. The released concentration is higher than the exposure limit of Immediately Dangerous to Life and Health (IDLH) 300 ppm. In summary, results show that the most dangerous occurs during the first 25 minutes after ammonia release. This analysis was performed for each season of the year and distances. Furthermore, Table 5 summarizes the results indicating the maximum distance of the three zones and all seasons.

3.3.2 Scenario 2: Flammable Area (Flash fire)

The objective of this scenario is to determine concentration estimates at the point downwind, distances of the flammability threat zone, and direction of the flammable area of the vapor cloud during an accident. The flammable area footprint of ammonia cloud zones at risk of fire is shown in Figure 5. The two zones are depicted with two colors: the red zone represents ammonia concentrations over 90,000 ppm—matching LOC-3 level (i.e., 60% of the LEL) with flame pockets—while the yellow zone signifies concentrations exceeding 15,000 ppm, corresponding to LOC-1 level (i.e., 10% LEL of ammonia). Figure 5 and Table 5 also show that the risk is limited to a distance of 368 meters from the source in the red zone and yellow zone, a distance of 893 meters, and the red zone has a high risk of fire and threat at blue point have concentration estimates at the point downwind 100 meters. It has a maximum concentration outdoors, as shown by the red line in Figure 5. The forecasted flammable vapors are 505,000 ppm, exceeding 60% LEL during the first 5 minutes after the ammonia release, and the blue line forecasted concentration indoors does not reach the LOC-1 level with 6,280 ppm; however, concentration in the blue line does not exceed LOC-1 level, but high concentration effected to people a wide area shows in Figure 5.

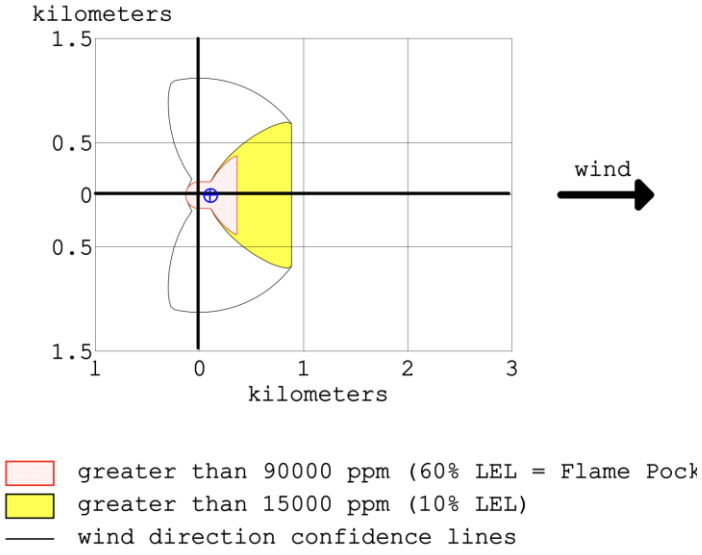

Figure 5. Distances of ammonia flammable threat zone (flash fire).

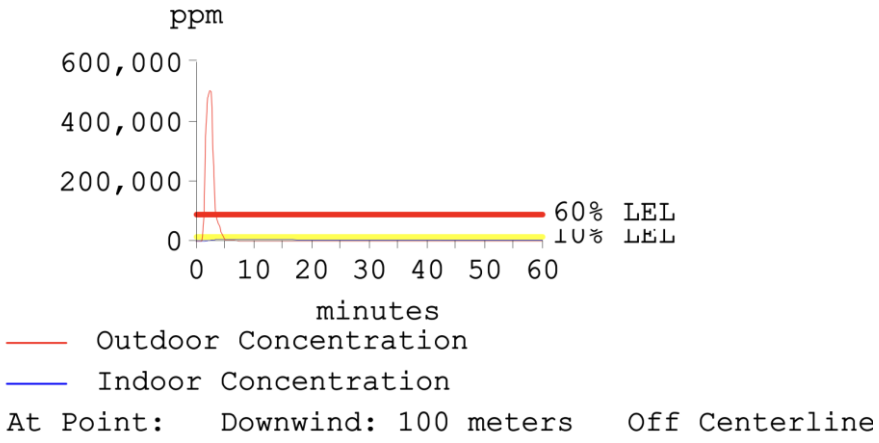

Figure 6. Concentration at point flammable area (flash fire).

3.3.3 Scenario 3: Flammable Area (Jet fire)

This scenario determines the thermal radiation of the jet fire. The jet fire modeling involved calculating thermal radiation measured in kW/m² using a specialized jet fire model. In this context, thermal radiation represents the heat energy emitted by the jet fire source. The thermal radiation at 110 meters from the most distant jet fire source within the yellow zone was determined to be 2.0 kW/m². This value suggests that the thermal radiation at that distance can induce pain within 60 seconds due to its intensity. Thermal radiation estimates that the blue point at the orange zone was determined to be 5.0 kW/m². Thermal radiation at 64 meters might cause 2-degree burns within 60 seconds. The red zone is 10.0 kW/m², so it can potentially be lethal within 60 seconds, and given the high population density, an accident could result in a catastrophic event leading to a significant loss of life. Within 2 min after ammonia release, jet fire has thermal radiation to second-degree burn and pain, and the maximum thermal radiation is 7.02 kW/m², as shown in Figure 7, 8. It is noteworthy that ammonia, in this scenario, exhibits a thermal radiation distance of 110 meters. The farthest distance from the source of the jet fire, as illustrated in Figure 7, is established to be 110 meters during the summer. This information is crucial for assessing the potential heat impact on surrounding areas and structures, aiding in developing safety measures and emergency response plans to mitigate the consequences of an ammonia jet fire incident.

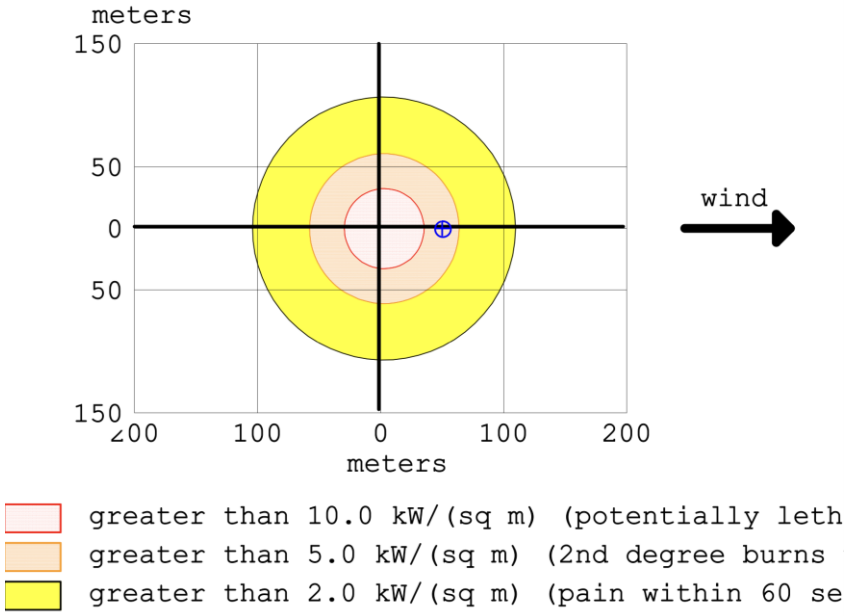

Figure 7. Distances of thermal radiation threat zone jet fire.

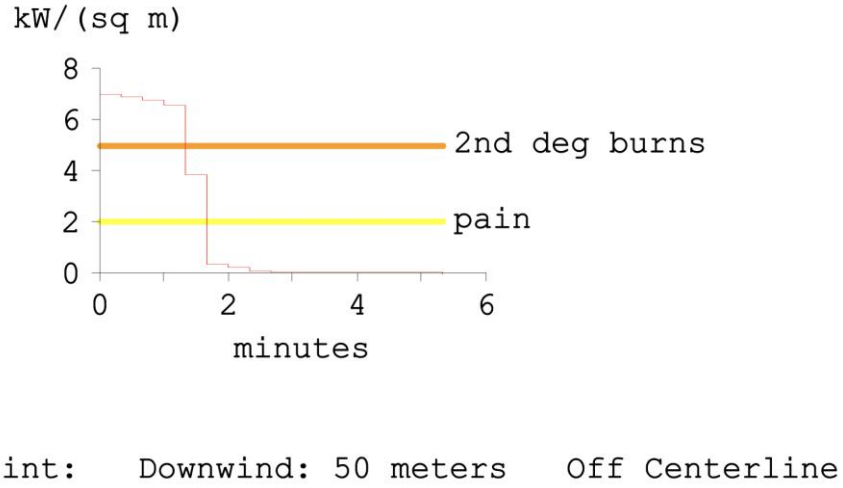

Figure 8. Thermal radiation at point jet fire.

3.3.4 Scenario 4: BLEVE (Fireball)

This scenario determines the thermal radiation from the fireball. Results from the ammonia BLEVE modeling were calculated using the fireball model. The fireball model calculates the dynamics of the fireball, including its size and shape, based on factors such as ammonia release rate, initial conditions, and environmental variables. Additionally, the model helps estimate the range of thermal radiation the fireball produces, which is critical for assessing potential damage to structures and the risk to individuals in the vicinity. The calculated thermal radiation at a specific distance, precisely 207 meters from the closest BLEVE source in the red zone, was determined to be 10.0 kW/m^2. This value indicates the intensity of the thermal radiation at that distance can be potentially lethal within 60 seconds. The orange zone, which is 301 meters, might cause 2-degree burns within 60 seconds. The yellow zone thermal radiation at a specific distance, precisely 476 meters from the farthest jet fire source, was determined to be 2.0 kW/m^2. This value indicates the intensity of the thermal radiation at that distance can cause pain within 60 seconds. As shown in Figure 9, the estimated thermal radiation reaches a maximum of 28.8 kW/m^2 at that point, featuring a fireball 152 meters in diameter and lasting 10 seconds.

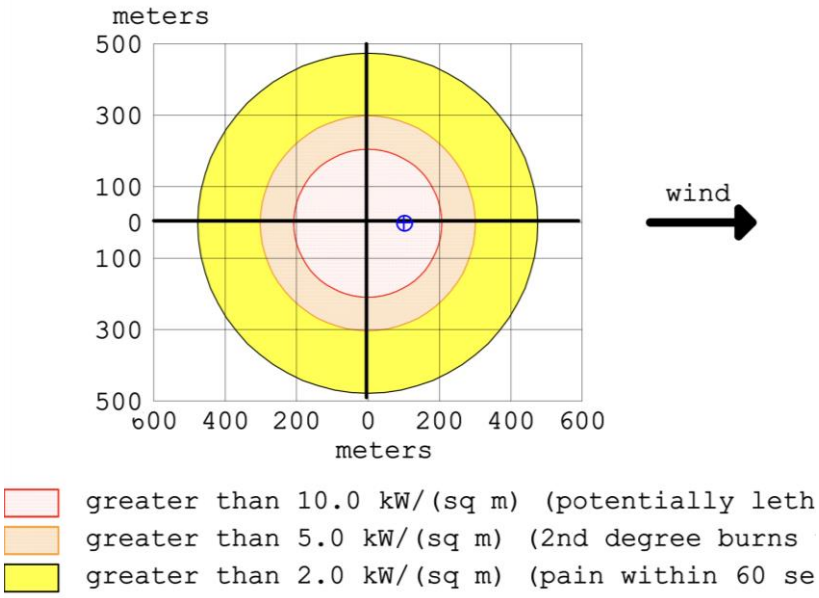

Figure 9. Distances of thermal radiation threat zone BLEVE (fireball).

3.3.5 Scenario 5: Vapor Cloud Explosion (VCE)

This scenario determines the ammonia cloud's overpressure (blast force) threat zone, which is estimated using the ammonia VCE model as an empirical model. The blast forces from the vapor cloud explosion in the yellow zone were 639 meters from the farthest VCE source at LOC-1 with 1.0 psi can a shattered glass, and the orange zone simulated pressure was 3.5 psi is serious injury likely with distances of 364 meters. The red zone was determined to have an overpressure blast force of 8.0 psi, which destroyed buildings at distances of 310 meters. This scenario has a release duration of 5 minutes and a maximum average sustained release rate of 11,200 kilograms/min (averaged over a minute or more). The total amount released is 16,970 kilograms. Threat at point downwind 100 meters has an overpressure estimate at the point with an overpressure of 293 psi, exceeding LOC-3 8.0 psi. The explosion was violent enough to destroy buildings. Blast forces of ammonia, highest at distances more than 630 m in the rainy season, are presented in Figure 10. Table 5 shows data distances from accident point sources in all five scenarios and seasons.

According to the main results of scenario 1 in summer, red, orange, and yellow threat distances were found to be 2.4 km, 4.8 km, and 8.9 km downwind, respectively. Compared with other seasons, such as rainy, red, orange, and yellow, threat distances were 2.5 km, 4.5 km, and 8.9 km, respectively. The winter in the red, orange, and yellow threat distances were found to be 2.4 km, 4.9 km, and 8.9 km downwind, respectively ,

finding that the distance in the yellow zone in the three seasons was no different. In Scenario 2, the ammonia-induced fire poses the highest risk at 368 meters from the accident source's red zone (60% LEL) during summer. During the rainy and winter seasons, the limited fire risk is approximately the same at 358 meters and 359 meters, respectively, and in other scenarios, the distances do not differ significantly. This indicates that ammonia transportation accidents under strong meteorological conditions can enable poisonous gas to travel long distances quickly, negatively affecting social life and the economy. Evaluate the risks associated with ammonia transportation and the possible undesirable consequences of any truck accident leak or rupture. As examples from the previous studies, the consequences of possible accidents were determined using the ALOHA program.

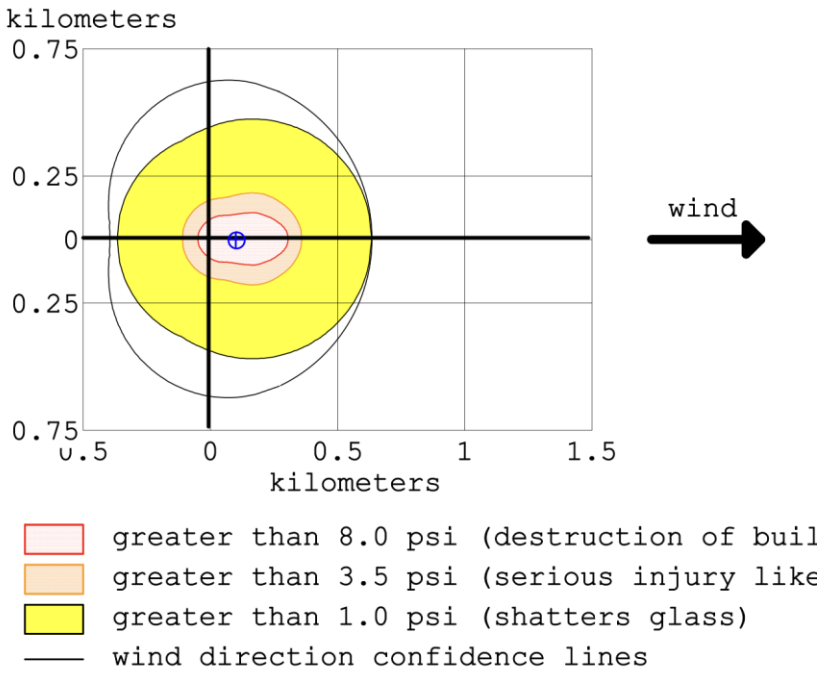

Figure 10. Distances of overpressure (blast force) threat zone.

Table 6 summarizes the most dangerous circumstances in the accident of ammonia transportation for the six study points. The most dangerous moment of ammonia concentration outdoors in scenario 1 is 505,000 ppm during the first 5 minutes after the release. Point 2 350 meters concentration 97,500 ppm during the first 10 minutes after the release. The data indicate that outdoor concentrations in scenarios 1 and 2 exceed the EPA's highest toxicity level (AEGL-3). An indoor LOC-3 (AEGL-3) concentration is observed at point 2, while concentrations at points 3 to 6 surpass AEGL-1. The maximum outdoor concentrations in scenarios 1 and 2 are consistent across all seasons due to identical data inputs and simulated results. Previous studies also indicated that the toxic vapor cloud scenario resulted in the most hazardous situation [23, 31].

The consequences modeling of various accident outcomes, a dispersion of toxic vapor cloud will move in a downwind direction and spread in a crosswind. In the case of ammonia, the intensity of heat radiation in scenario 3 flammable area (jet fire) is the least, not exceeding LOC-2 (5 kW/m^2) point 1 maximum intensity with 2.39 kW/m^2. This may be not only due to low heat of combustion and vaporization values but also to intensity greater than 2.0 kW/m^2, which can cause pain within 60 seconds. Figure 7 shows the toxic threat zone, thermal threat zone, and overpressure (blast force) threat zone of ammonia created by toxic vapor cloud, BLEVE, and VCE that is superimposed and visualized in the Google Earth map [43, 50]. The effect on the residents in the vicinity led to a domino effect.

Table 6. Summary of the most impact distances and maximum concentration of ammonia release on all scenarios.

Season	Distance from the emission source (m)	Max concentration outdoor					Max concentration indoor		Most dangerous moment
		Scenario 1: Toxic Vapor Cloud (ppm) (AEGL -3)	Scenario 2: Flammable area (Flash Fire) (ppm) (60% LEL)	Scenario 3: Flammable area (Jet Fire) (kW/m²)	Scenario 4: BLEVE (Fireball) (kW/m²)	Scenario 5: Vapor Cloud Explosion (psi)	Scenario 1: Toxic Vapor Cloud (ppm) (AEGL-1)	Scenario 2: Flammable area (Flash Fire) (ppm) (10% LEL)	
Summer	Point 1 100	505,000	505,000	2.390	28.800	293	6,270	6,280	First 5 min. after the release
	Point 2 350	97,500	97,500	0.187	3.720	4.040	1,620	1,620	The first 10 min. after the
	Point 3 500	51,600	51,600	0.088	1.810	1.560	1,060	1,060	The first 10 min. after the
	Point 4 1,000	11,600	11,600	0.020	0.428	0.498	379	380	First 20 min. after the release
	Point 5 1,500	4,180	4,180	0.009	0.182	0.283	183	183	First 25 min. after the release
	Point 6 2,100	1,680	1,680	0.004	0.089	0.182	94	95	First 35 min. after the release
Rainy	Point 1 100	497,000	497,000	2.320	28.100	293	6,170	6,180	First 5 min. after the release
	Point 2 350	93,200	93,200	0.182	3.610	3.820	1,610	1,610	The first 10 min. after the
	Point 3 500	49,600	49,600	0.085	1.760	1.530	1,060	1,060	The first 10 min. after the
	Point 4 1,000	11,600	11,600	0.020	0.414	0.490	398	399	First 20 min. after the release
	Point 5 1,500	4,270	4,280	0.008	0.176	0.279	197	197	First 25 min. after the release
	Point 6 2,100	1,740	1,740	0.004	0.086	0.180	103	104	First 35 min. after the release
Winter	Point 1 100	508,000	508,000	2.250	28	293	6,120	6,130	First 5 min. after the release
	Point 2 350	93,800	93,800	0.176	3.590	3.870	1,560	1,560	The first 10 min. after the
	Point 3 500	49,600	49,600	0.083	1.740	1.540	1,030	1,030	The first 10 min. after the
	Point 4 1,000	11,600	11,600	0.019	0.411	0.472	385	386	First 20 min. after the release
	Point 5 1,500	4,240	4,240	0.008	0.175	0.269	190	191	The first 30 min. after the
	Point 6 2,100	1,720	1,730	0.004	0.085	0.174	99	100	First 35 min. After the release

Considering the location and distance of the threat zone, the areas most affected by the accidental release are Chamai and Khonkrot; therefore, these areas were selected for the vulnerability study. Vulnerable groups, such as children under 5 and elderly individuals over 65, exhibit varying sensitivity to ammonia, affecting their ability to escape the threat zone promptly [16]. People with heart illness, physical limitations, and respiratory system problems. This is consistent with the findings of [25] study on impaired lung function. This impairs the person's ability to respond in areas such as vision, hearing, and perception. Intellectual disabilities may limit comprehension of the issue, or a disabled person may be unable to seek assistance from a career in an emergency. Being more sensitive to ammonia, vulnerable populations face higher risks than the general public when accidents occur along ammonia transport routes. Exposure to ammonia is more severe than in people with perfect health. In addition to the aligned study [32], results reflect that the residents residing in highly populated areas near the accidental site tend to be more vulnerable. In the event of an ammonia transportation accident in Thungsong, a risk map is utilized to protect and prevent impact on the local population. According to simulated results, meteorological variations demonstrate that wind directions are northeast in summer and winter and shift to southwest during the rainy season. These wind directions directly impact the neighborhoods located nearby. Accidental ammonia releases on roads will significantly affect a high percentage of the surrounding population, causing adverse effects on human health, the environment, and properties close to the accident site.

3.4 GIS mapping

3.4.1 Severity, risk, and evacuation route maps

The severity of accidental ammonia transportation mapping within the threat zone is assessed using ArcGIS. It provides necessary information about the population vicinity of the threat zone. When the source point of an accident has a population density exceeding 12,000 inhabitants, the threat zone identified to the area may directly affect and severely impact the population and cover economic and vulnerable areas with a population density of more than 30,000 inhabitants, as shown in Figure 11. Risk map Figure 12 shows the radius of the spread of overpressure corresponding to 10 kW/m^2, the largest for ammonia in summer and lowest in rainy and winter. It shows a distance of toxicity dispersion and flammable threat zone of radiation footprint. Superimposing layers prepare vulnerability and severity maps, consistent with this study by Rajeev et al. [43]. Study area, risk, and vulnerability maps were prepared using ArcGIS software. The risk measures the exposure probability of the population, vulnerable groups, and sensitive target places, such as hospitals, schools, residential areas, villages, temples, etc., to ammonia release.

ArcGIS can evaluate the spatial reach of different scenarios that may spread or disperse to nearby source points. The population in the surrounding area is also factored in, with higher population densities leading to increased severity. The severity map of the study area is shown in Figure 11. The sensitive targets placed within the study area are identified, and their relative is assessed by overlay analysis. Then, population density, emergency services, and hospitals are identified and quantified. Population density serves as a measure of societal vulnerability, making densely populated areas in need of immediate attention during accidents. Residential regions with high population densities should be given priority in emergency preparedness strategies [32, 52, 53]. Risk mapping, also created by GIS in this study, overlaid the toxic threat zone, radiation threat zone, and overpressure threat zone map into a risk map that identified high-risk areas. The risk map can be used as a decision-making tool to prepare emergency plans and land use planning, which might decrease the impact of the ammonia transportation accident in the future. Chau et al. created a risk map for the entire facility, with traffic light colors serving as danger indications [54]. Developed a methodology for risk management and emergency decision-making of offshore oil spill accidents, which is implemented with Bayesian by Li et al. [55]. Hence, evacuation mapping uses decision-making to prepare evacuation routes or response plans that identify safety points and areas that can be used as assembly points and emergency services if the accident risk is significant. The network analysis technique of GIS is used to design buffer zones for such accidents. Buffer areas identified are 3 schools, 4 hospitals, 2 temples, and five villages located in unacceptable risk areas, as shown in Figure 13.

In conclusion, severity, risk, and evacuation route maps are vital components of emergency preparedness and response, delivering critical information to decision-makers, emergency personnel, and the

public, such as in a small spill, initially isolating individuals within 30 meters of the affected area. Maintain a distance of 100 meters during daylight hours and 200 meters at night. Initially, individuals within 150 meters of the area should be isolated for a large spill. Maintain an 800-meter distance during the day and 2,300 meters at night. Utilizing these maps effectively enables communities to strengthen their resilience, decrease the impact of disasters, and save lives during urgent situations. ArcGIS plays a fundamental role in producing comprehensive risk maps for emergency management by combining spatial data, conducting hazard assessments, evaluating vulnerabilities, analyzing risks, and aiding decision-making processes. With ArcGIS technology, emergency planners can enhance risk assessments, optimize response strategies, and implement resilience-building measures, thereby improving community safety and minimizing disaster repercussions.

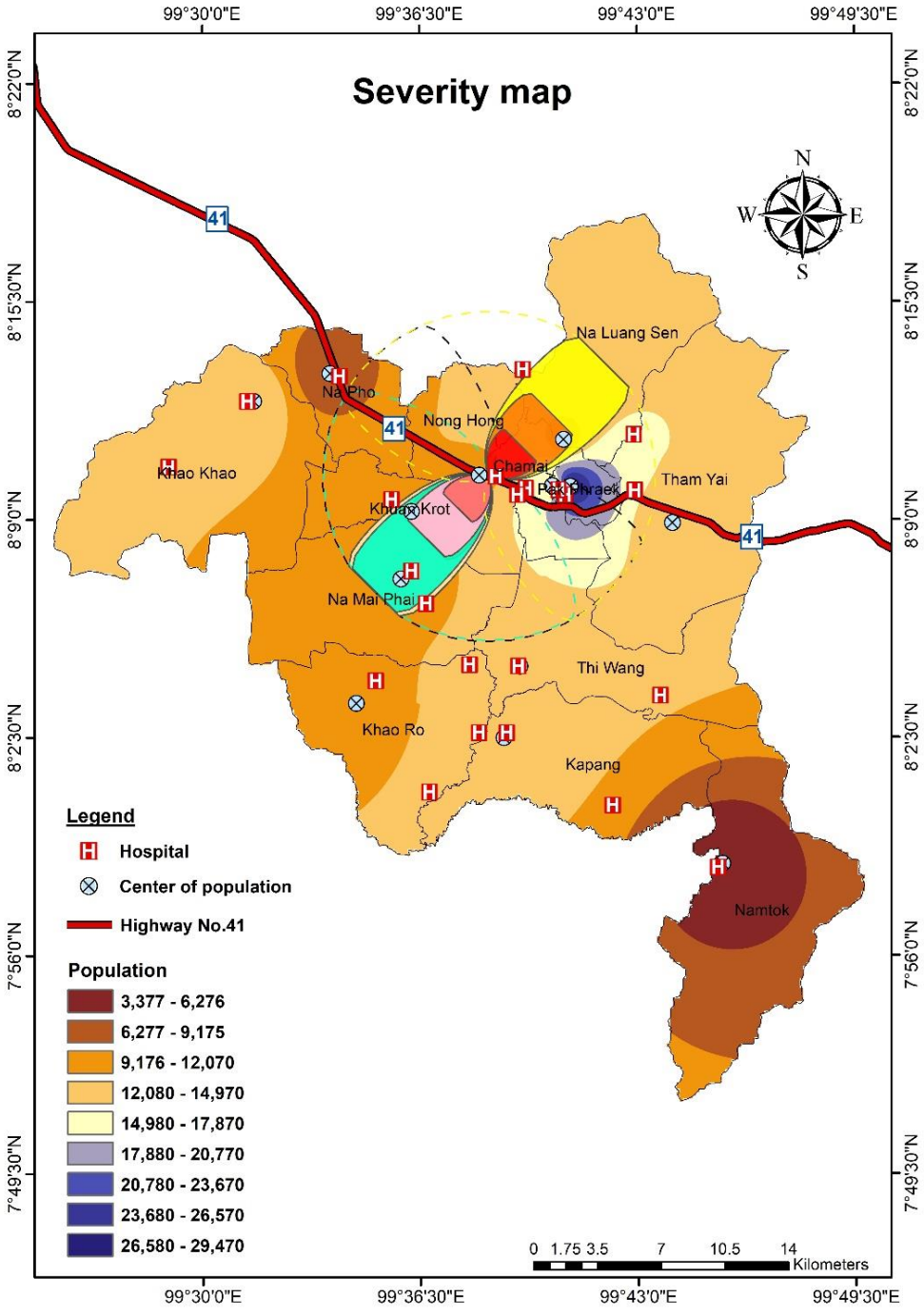

Figure 11. Severity map.

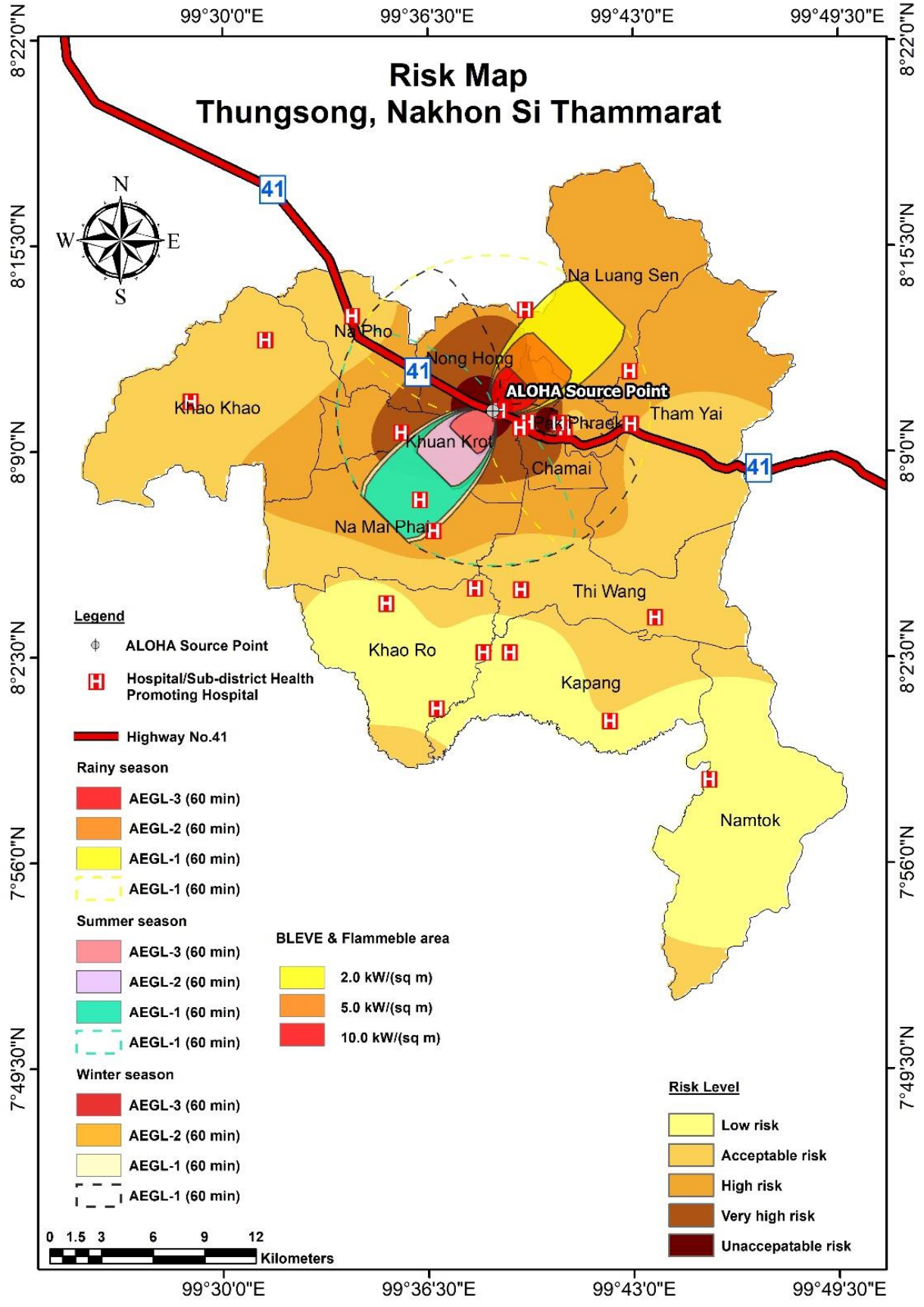

Figure 12. Risk map of the studied area.

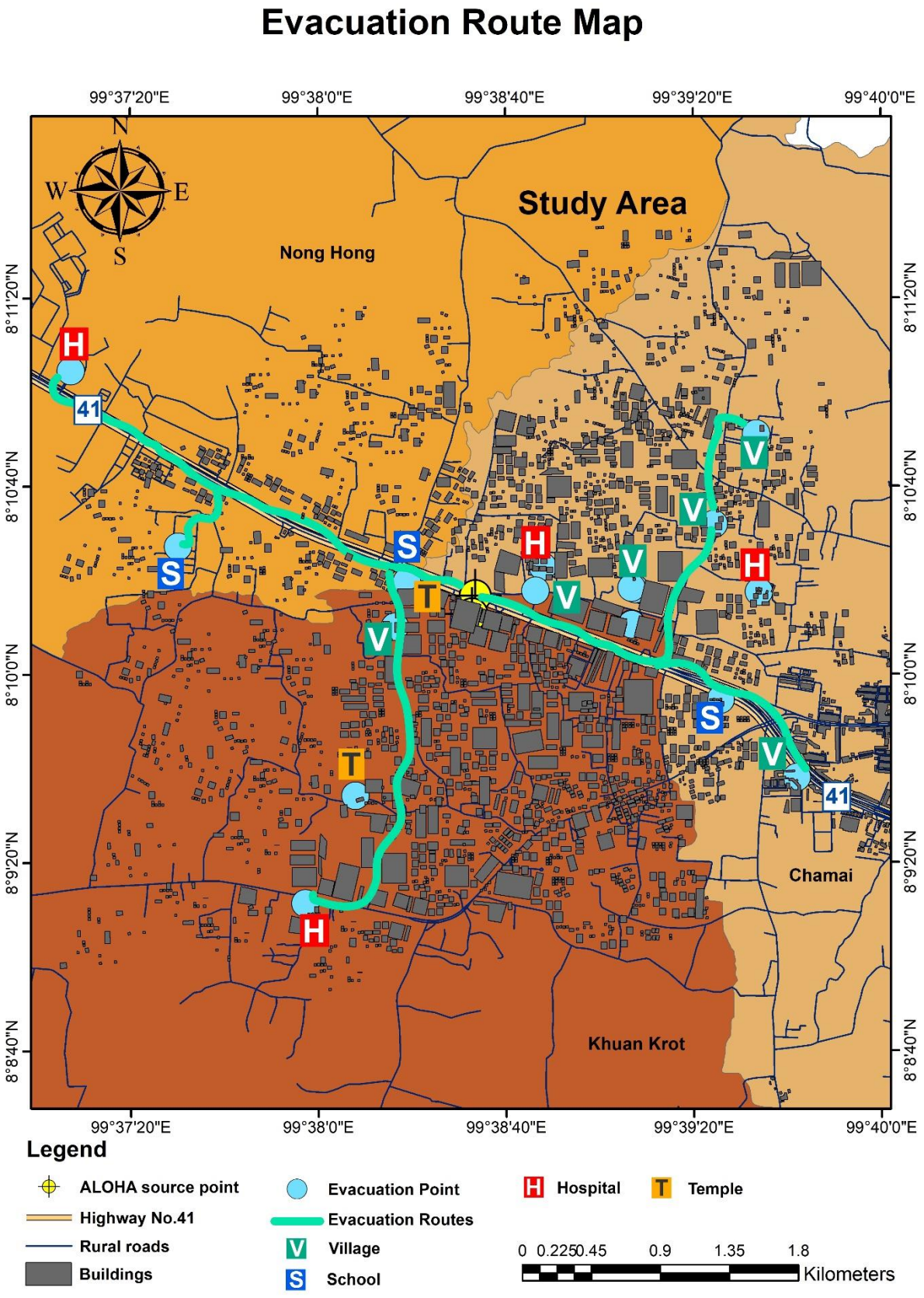

Figure 13. Evacuation map of the studied area.

4. Conclusions

This study assessed ammonia emission risks in a densely populated area by overlaying ALOHA results onto ArcGIS to create threat zone maps. In scenario 1, the red danger zone extends 2,400 meters from the source, with ammonia levels reaching up to 505,000 ppm, while in scenario 2, the red zone spans 368 meters. Explosive hazards (BLEVE and VCE) have ranges of 207 and 310 meters, respectively. In Thungsong, areas including 3 schools, 4 hospitals, 2 temples, and 5 villages are in unacceptable risk zones, exposing residents to ammonia levels exceeding 1,100 ppm, posing severe health risks. The study highlights the need for safety measures, evacuation plans, and continuous training to protect vulnerable populations and critical infrastructure. Future work should include real-time meteorological data to improve ammonia dispersion accuracy and adapt risk assessments for climate change impacts. The maps created are essential tools for emergency response planning and decision-making. Developing detailed evacuation maps and risk assessment tools is essential for effective emergency response within emergency plans. Moreover, implementing ongoing training programs and emergency drills for local authorities and communities can increase readiness and expedite response times. A limitation of this research is its reliance on static risk maps that do not account for real-time changes in environmental conditions, population movements, or ammonia dispersion patterns, which can vary with weather and other dynamic factors. This limits the ability to provide timely, adaptable responses during an actual ammonia release incident, highlighting the need for dynamic, real-time risk mapping in future studies.

5. Acknowledgements

The authors thank the School of Public Health, Walailak University (Grant No. 01/2564 & 01/2565) for the financial support.

Authorship contributions: Conceptualization: P.K.; methodology: P.K., S.Y., P.S., and J.M.; software: P.K.; validation: P.K.; formal analysis: P.K.; investigation: P.K.; data curation: P.K.; writing-original draft preparation: P.K.; writing - review and editing: S.Y., P.S., and J.M.; visualization: P.K.; supervision: J.M.; project administration: J.M. All authors have read and agreed to the published version of the manuscript.

Funding: This research was supported by the School of Public Health, Walailak University (Grant No. 01/2564 & 01/2565)

Conflicts of Interest: The authors declare no conflict of interest.

References

[1] Jabbari, M.; Atabi, F.; Ghorbani, R., Key airborne concentrations of chemicals for emergency response planning in HAZMAT road transportation- margin of safety or survival. *Journal of Loss Prevention in The Process Industries* **2020,** *65*, 104139.

[2] Bondžić, J.; Sremački, M.; Popov, S.; Mihajlović, I.; Vujić, B.; Petrović, M., Exposure to hazmat road accidents - Toxic release simulation and GIS-based assessment method. *J Environ Manage* **2021,** *293*, 112941.

[3] Fan, T.; Chiang, W.-C.; Russell, R., Modeling urban hazmat transportation with road closure consideration. *Transportation Research Part D: Transport and Environment* **2015,** *35*, 104-115.

[4] Brzozowska, L., Computer simulation of impacts of a chlorine tanker truck accident. *Transportation research part D: transport and environment* **2016,** *43*, 107-122.

[5] Inanloo, B.; Tansel, B., Explosion impacts during transport of hazardous cargo: GIS-based characterization of overpressure impacts and delineation of flammable zones for ammonia. *Journal of Environmental Management* **2015,** *156*, 1-9.

[6] Ghaleh, S.; Omidvari, M.; Nassiri, P.; Momeni, M.; Lavasani, S., Pattern of safety risk assessment in road fleet transportation of hazardous materials (oil materials). *Safety Science* **2019,** *116*, 1-12.

[7] Vianello, C.; Maschio, G., Quantitative risk assessment of the Italian gas distribution network. *Journal of Loss Prevention in the Process Industries* **2014,** *32*, 5-17.

[8] Bubbico, R.; Maschio, G.; Mazzarotta, B.; Milazzo, M. F.; Parisi, E., Risk management of road and rail transport of hazardous materials in Sicily. *Journal of Loss Prevention in the Process Industries* **2006,** *19*(1), 32-38.
[9] Fabiano, B.; Currò, F.; Palazzi, E.; Pastorino, R., A framework for risk assessment and decision-making strategies in dangerous good transportation. *Journal of Hazardous Materials* **2002,** *93*(1), 1-15.
[10] Egidi, D.; Foraboschi, F. P.; Spadoni, G.; Amendola, A., The ARIPAR project: analysis of the major accident risks connected with industrial and transportation activities in the Ravenna area. *Reliability Engineering & System Safety* **1995,** *49*(1), 75-89.
[11] Bouet, R.; Duplantier, S.; Salvi, O., Ammonia large scale atmospheric dispersion experiments in industrial configurations. *Journal of Loss Prevention in the Process Industries* **2005,** *18*(4), 512-519.
[12] Junior, M. M.; e Santos, M. S.; Vidal, M. C. R.; de Carvalho, P. V. R., Overcoming the blame game to learn from major accidents: A systemic analysis of an Anhydrous Ammonia leakage accident. *Journal of loss prevention in the process industries* **2012,** *25*(1), 33-39.
[13] Tan, W.; Du, H.; Liu, L.; Su, T.; Liu, X., Experimental and numerical study of ammonia leakage and dispersion in a food factory. *Journal of Loss Prevention in the Process Industries* **2017,** *47*, 129-139.
[14] Yarandi, M. S.; Mahdinia, M.; Barazandeh, J.; Soltanzadeh, A., Evaluation of the toxic effects of ammonia dispersion: consequence analysis of ammonia leakage in an industrial slaughterhouse. *Medical gas research* **2021,** *11*(1), 24.
[15] Gangopadhyay, R.; Das, S., Ammonia leakage from refrigeration plant and the management practice. *Process Safety Progress* **2008,** *27*(1), 15-20.
[16] Sanchez, E. Y.; Represa, S.; Mellado, D.; Balbi, K. B.; Acquesta, A. D.; Colman Lerner, J. E.; Porta, A. A., Risk analysis of technological hazards: Simulation of scenarios and application of a local vulnerability index. *Journal of Hazardous Materials* **2018,** *352*, 101-110.
[17] Roney, N.; Llados, F., Toxicological profile for ammonia. **2004**.
[18] Sekizawa, S.-i.; Tsubone, H., Nasal receptors responding to noxious chemical irritants. *Respiration physiology* **1994,** *96*(1), 37-48.
[19] Bai, Z.; Dong, Y.; Wang, Z.; Zhu, T., Emission of ammonia from indoor concrete wall and assessment of human exposure. *Environment international* **2006,** *32*(3), 303-311.
[20] Cheng, J.; Shen, J.; Jia, L.; Hu, K. In *Simulation analysis of the influence of leakage location and flow rate on the leakage of liquid ammonia tank*, International Conference on Computational Modeling, Simulation, and Data Analysis (CMSDA 2021), SPIE: **2022**, 232-236.
[21] Inanloo, B.; Tansel, B.; Jin, X.; Bernardo-Bricker, A., Cargo-specific accidental release impact zones for hazardous materials: risk and consequence comparison for ammonia and hydrogen fluoride. *Environment Systems and Decisions* **2016,** *36*(1), 20-33.
[22] NIOSH, Ammonia: Exposure Routes and Symptoms. **2019**.
[23] Orozco, J. L.; Caneghem, J. V.; Hens, L.; González, L.; Lugo, R.; Díaz, S.; Pedroso, I., Assessment of an ammonia incident in the industrial area of Matanzas. *Journal of Cleaner Production* **2019,** *222*, 934-941.
[24] Tan, W.; Lv, D.; Guo, X.; Du, H.; Liu, L.; Wang, Y., Accident consequence calculation of ammonia dispersion in factory area. *Journal of Loss Prevention in the Process Industries* **2020,** *67*, 104271.
[25] Tepper, A.; Comstock, G. W.; Levine, M., A longitudinal study of pulmonary function in fire fighters. *American journal of industrial medicine* **1991,** *20*(3), 307-316.
[26] George, A.; Bang, R. L.; Lari, A.-R.; Gang, R. K.; Kanjoor, J. R., Liquid ammonia injury. *Burns* **2000,** *26*(4), 409-413.
[27] Montague, T. J.; Macneil, A. R., Mass ammonia inhalation. *Chest* **1980,** *77*(4), 496-498.
[28] Rahman, N.; Ansary, M. A.; Islam, I., GIS based mapping of vulnerability to earthquake and fire hazard in Dhaka city, Bangladesh. *International Journal of Disaster Risk Reduction* **2015,** *13*, 291-300.
[29] Bariha, N.; Mishra, I. M.; Srivastava, V. C., Fire and explosion hazard analysis during surface transport of liquefied petroleum gas (LPG): a case study of LPG truck tanker accident in Kannur, Kerala, India. *Journal of loss prevention in the process industries* **2016,** *40*, 449-460.

[30] Chakrabarti, U. K.; Parikh, J. K., Route risk evaluation on class-2 hazmat transportation. *Process Safety and Environmental Protection* **2011,** *89*(4), 248-260.
[31] Anjana, N.; Amarnath, A.; Nair, M. H., Toxic hazards of ammonia release and population vulnerability assessment using geographical information system. *Journal of environmental management* **2018,** *210*, 201-209.
[32] Li, F.; Bi, J.; Huang, L.; Qu, C.; Yang, J.; Bu, Q., Mapping human vulnerability to chemical accidents in the vicinity of chemical industry parks. *Journal of Hazardous Materials* **2010,** *179*(1), 500-506.
[33] NOAA, E., ALOHA: USER'S MANUAL **2007**.
[34] Han, Z. Y.; Weng, W. G., Comparison study on qualitative and quantitative risk assessment methods for urban natural gas pipeline network. *Journal of Hazardous Materials* **2011,** *189*(1), 509-518.
[35] Patal, P.; Sohani, N., Hazard evaluation using ALOHA tool in storage area of an oil refinery. *International Journal of Research in Engineering and Technology* **2015,** *4*(12), 204-209.
[36] Khan, F. I.; Abbasi, S. A., An assessment of the likelihood of occurrence, and the damage potential of domino effect (chain of accidents) in a typical cluster of industries. *Journal of Loss Prevention in the Process Industries* **2001,** *14*(4), 283-306.
[37] AlRukaibi, F.; Alrukaibi, D.; Alkheder, S.; Alojaiman, S.; Sayed, T., Optimal route risk-based algorithm for hazardous material transport in Kuwait. *Journal of Loss Prevention in the Process Industries* **2018,** *52*, 40-53.
[38] Anjana, N.; Amarnath, A.; Chithra, S.; Harindranathan Nair, M.; Jose, S. K., Population vulnerability assessment around a LPG storage and distribution facility near Cochin using ALOHA and GIS. *International Journal of Engineering Science Invention* **2015,** *4*(6), 23-31.
[39] Meysami, H.; Ebadi, T.; Zohdirad, H.; Minepur, M., Worst-case identification of gas dispersion for gas detector mapping using dispersion modeling. *Journal of Loss Prevention in the Process Industries* **2013,** *26*(6), 1407-1414.
[40] Hu, T.; Xiong, J.; Zhou, J.; Xia, Q., Nitrogen removal performance of bioretention cells under freeze-thaw cycles: Effects of filler structure and microbial community. *Journal of Environmental Management* **2024,** *369*, 122380.
[41] Zhou, J.; Xiong, J.; Zhu, J.; Xie, X.; Ni, J.; Liu, Y.; Wang, X., Effects of freeze-thaw cycles on nutrient removal from bioretention cells. *Journal of Environmental Management* **2023,** *325*, 116556.
[42] Khanmohamadi, M.; Bagheri, M.; Khademi, N.; Ghannadpour, S. F., A security vulnerability analysis model for dangerous goods transportation by rail – Case study: Chlorine transportation in Texas-Illinois. *Safety Science* **2018,** *110*, 230-241.
[43] Rajeev, K.; Soman, S.; Renjith, V. R.; George, P., Human vulnerability mapping of chemical accidents in major industrial units in Kerala, India for better disaster mitigation. *International journal of disaster risk reduction* **2019,** *39*, 101247.
[44] Besiktas, R.; Baltaci, H.; Akkoyunlu, B. O., Simulation of the Jet Fire Using Atmospheric Dispersion Modeling (ALOHA): A Case Study of Natural Gas Pipeline in Istanbul, Türkiye. *Atmosphere* **2024,** *15*(4), 456.
[45] Jirsa, P., An Analysis of the Cumulative Uncertainty Associated with a Quantitative Consequence Assessment of a Major Accident. *Process Safety and Environmental Protection* **2007,** *85* (3), 256-259.
[46] Griffiths, R. F., The use of probit expressions in the assessment of acute population impact of toxic releases. *Journal of Loss Prevention in the Process Industries* **1991,** *4*(1), 49-57.
[47] Zhou, Y.; Hu, G.; Li, J.; Diao, C., Risk assessment along the gas pipelines and its application in urban planning. *Land Use Policy* **2014,** *38*, 233-238.
[48] Duijm, N. J.; Markert, F.; Paulsen, J. L., *Safety assessment of ammonia as a transport fuel*. Risø National Laboratory: 2005.
[49] Gyenes, Z.; Wood, M. H.; Struckl, M., *Handbook of scenarios for assessing major chemical accident risks*. Publications Office of the European Union: 2017.
[50] Zhang, D.; Mao, Z.; Gong, M.; Ren, J.; Zuo, S.; Chen, X., Study on optimization of shelter locations and evacuation routes of gas leakage accidents in chemical industrial park. *Process Safety and Environmental Protection* **2023,** *177*, 556-567.

[51] Lee, H. E.; Sohn, J.-R.; Byeon, S.-H.; Yoon, S. J.; Moon, K. W., Alternative risk assessment for dangerous chemicals in South Korea regulation: Comparing three modeling programs. *International journal of environmental research and public health* **2018,** *15*(8), 1600.

[52] Tahmid, M.; Dey, S.; Syeda, S. R., Mapping human vulnerability and risk due to chemical accidents. *Journal of Loss Prevention in the Process Industries* **2020,** *68*, 104289.

[53] Sengupta, A.; Bandyopadhyay, D.; Roy, S.; van Westen, C. J.; van der Veen, A., Challenges for introducing risk assessment into land use planning decisions in an Indian context. *Journal of Loss Prevention in the Process Industries* **2016,** *42*, 14-26.

[54] Chau, K.; Djire, A.; Vaddiraju, S.; Khan, F., Process Risk Index (PRI) – A methodology to analyze the design and operational hazards in the processing facility. *Process Safety and Environmental Protection* **2022,** *165*, 623-632.

[55] Li, X.; Zhu, Y.; Abbassi, R.; Chen, G., A probabilistic framework for risk management and emergency decision-making of marine oil spill accidents. *Process Safety and Environmental Protection* **2022,** *162*, 932-943.